# Quantized Current in a Quantum-Dot Turnstile Using Oscillating Tunnel Barriers

L. P. Kouwenhoven, A. T. Johnson, N. C. van der Vaart, and C. J. P. M. Harmans
*Faculty of Applied Physics, Delft University of Technology, P.O. Box 5046, 2600GA Delft, The Netherlands*

C. T. Foxon
*Philips Research Laboratories, Redhill, Surrey RH15HA, United Kingdom*
(Received 20 May 1991)

We have observed a quantized current in a lateral quantum dot, defined by metal gates in the two-dimensional electron gas (2DEG) of a GaAs/AlGaAs heterostructure. By modulating the tunnel barriers in the 2DEG with two phase-shifted rf signals, and employing the Coulomb blockade of electron tunneling, we produced quantized current plateaus in the current-voltage characteristics at integer multiples of $ef$, where $f$ is the rf frequency. This demonstrates that an integer number of electrons pass through the quantum dot each rf cycle.

PACS numbers: 73.20.Dx, 06.20.Hq, 72.20.Fr, 73.40.Gk

The discreteness of the electron charge can cause dramatic transport phenomena in submicron structures. These single-electron charging effects have been studied in granular films, metal tunnel junctions, and scanning-tunneling-microscope–grain junctions [1], and more recently in semiconductor systems [2]. rf studies in conjunction with charging effects have been performed by Geerligs *et al.* [3], who applied a rf signal to the central island of a sample of four metal tunnel junctions in series. They observed a plateau at a current $I=ef$, with $f$ the frequency of the rf signal, demonstrating that exactly one electron per rf cycle passed through their so-called *turnstile* device. In a three-junction geometry, Pothier *et al.* [4] used two phase-shifted rf signals to realize a single-electron *pump*: a device with $I=ef$ at zero bias voltage.

Here we present the realization of a turnstile operation in a semiconductor quantum dot, defined by metal gates in a two-dimensional electron gas (2DEG). In contrast to metal systems, our quantum-dot turnstile relies on the ability to induce oscillating tunnel barriers between the quantum dot and the wide 2DEG regions by applying rf signals to the gates. The inset of Fig. 3 is a scanning-electron-microscope photograph of the gate geometry, which is fabricated on top of a GaAs/AlGaAs heterostructure containing a 2DEG about 100 nm below the surface. The ungated 2DEG has a mobility of $2.3\times10^6$ $cm^2/Vs$ and an electron density of $1.9\times10^{15}$ $m^{-2}$ at 4.2 K. We denote gate $F$ as the finger gate, gates 1 to 4 as quantum-point-contact (QPC) gates, and gate $C$ as the center gate. In the experiments discussed in this Letter, we do not use QPC gates 3 and 4; these gates are grounded and have no effect on the 2DEG. Applying $-400$ mV to gates $F$, $C$, 1, and 2 depletes the electron gas underneath them and forms a quantum dot with a diameter of about 0.8 $\mu$m in the 2DEG. The narrow channels between gates 1 and $C$ and between 2 and $C$ are pinched off at this gate voltage. Electron transport occurs only through the constrictions induced by gates 1 and $F$ and by 2 and $F$, which couple the dot to the two wide 2DEG regions.

Charging effects become important when the gate voltages are such that the constrictions form tunnel barriers with conductances $G_1, G_2 \ll 2e^2/h$ [5]. The electrons in the dot are then strongly localized, so $N$, the number of electrons in the dot, is an integer. The electrostatic energy associated with the addition of one electron to the dot is the charging energy $E_C=e^2/C$, where $C=\sum_i C_i$ is the sum of the capacitances between the dot and the two 2DEG reservoirs and between the dot and the different gates [6,7]. The difference in electrochemical potential in the dot is [5] $\mu_d(N+1)-\mu_d(N)=E_{N+1}-E_N+e^2/C$. The electrochemical potential $\mu_d(N)$ denotes the minimal energy of the $N$th electron in the dot, and $E_N$ is the energy of the $N$th single-particle state relative to the bottom of the conduction band. In our quantum dot, the energy difference between the discrete states, $E_{N+1}-E_N \approx 2E_F/N \approx 0.03$ meV, is much smaller than the charging energy $e^2/C \approx 1$ meV [5]. We therefore neglect the discreteness of the energy states in the remainder of this Letter.

Quantitative calculations of transport properties through semiconductor quantum dots, including discrete energy states and charging effects, are described in Refs. [8–10]. A qualitative description can be obtained from the schematic potential landscape of Fig. 1. We begin with the case of static tunnel barriers, and later on consider barriers oscillating out of phase. Electron tunneling occurs when a charge state $\mu_d(N+1)$ lies between the electrochemical potentials of the reservoirs [$\mu_r < \mu_d(N+1) < \mu_l$], as in Fig. 1(a). Tunneling into the dot increases the number of electrons by one, corresponding to a change in the electrochemical potential of $\mu_d(N+1)-\mu_d(N)=e^2/C$. Tunneling out of the dot reduces the number and the electrochemical potential again, and a new electron can repeat this process. Tunneling is suppressed when $\mu_d(N) < \mu_l, \mu_r < \mu_d(N+1)$, which can be accomplished by moving the bottom of the conduction band in the dot by changing the voltage on the center gate. In this case, an extra electron would increase the

 © 1991 The American Physical Society

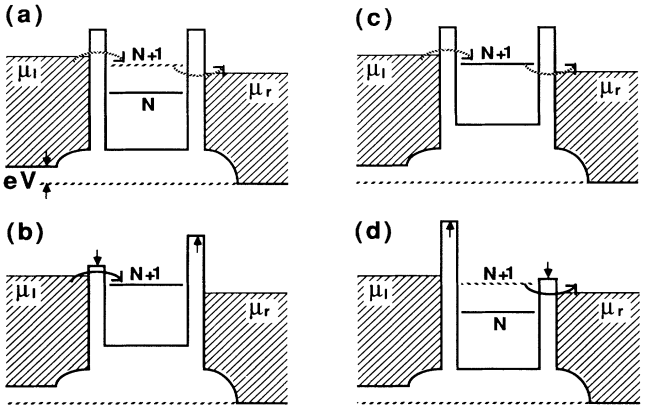


FIG. 1. Potential landscape through the quantum dot. $\mu_l$ and $\mu_r$ are the electrochemical potentials of the left and right reservoirs, and $V=(\mu_l-\mu_r)/e$ is the bias voltage. The level $N$ indicates $\mu_d(N)$ and $N$ electrons are confined in the quantum dot, while the level $N+1$ indicates $\mu_d(N+1)$. (a)–(d) are four stages of a rf cycle where the probability for electron tunneling is large when the barrier is low (solid arrows), and small when the barrier is high (dashed arrows).

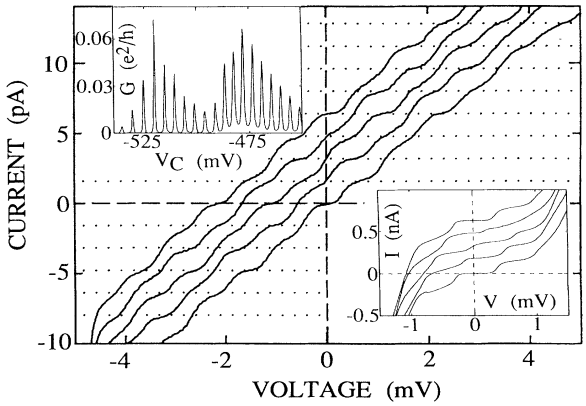


FIG. 2. Main figure: $I$-$V$ characteristics when two phase-shifted rf signals are applied with a frequency $f=10$ MHz, showing current plateaus at integer multiples of $ef$ (dotted lines). The curves correspond to different center-gate voltges and are offset for clarity by an integer times $ef$. Upper inset: Coulomb conductance oscillations vs center-gate voltage. Lower inset: Coulomb staircase in the $I$-$V$ characteristics (the curves correspond to different center-gate voltages and are offset for clarity).

electrochemical potential of the dot above the electrochemical potentials of the reservoirs. Such a tunnel event to a final state higher than the initial state is possible only by thermal activation or tunneling via virtual states [11]. This suppression of electron tunneling is known as the *Coulomb blockade.*

On varying the voltage on the center gate, the conductance $G$ of the dot is expected to oscillate between zero (Coulomb blockade) and nonzero (no Coulomb blockade). These *Coulomb oscillations* have recently been observed in quantum dots [2,12,13] and are shown in the upper inset of Fig. 2 for our sample. All measurements are performed at 10 mK and zero magnetic field. The Coulomb oscillations are measured with barrier conductances $G_1, G_2 \ll 2e^2/h$. The period of the oscillations is 4.6 mV, each period corresponding to a change of one electron in the dot.

For unequal tunnel barriers, a stepwise increase of the current $I$ upon increasing the bias voltage $V$ is expected [1,8,9]. A current step $\Delta I \approx eG/C$ occurs when the energy interval $eV$ between $\mu_l$ and $\mu_r$ contains an extra charge state. This *Coulomb staircase* is shown in the lower inset of Fig. 2. The five different curves correspond to different center-gate voltages: The lowest curve is at a minimum in the conductance oscillations, the curve in the middle at a conductance peak, and the uppermost curve at the next minimum. The width $\Delta V=0.67$ mV of the current plateaus is a direct measure of the charging energy: $e\Delta V=e^2/C$, from which we deduce the total capacitance $C=2.4\times10^{-16}$ F.

We now demonstrate that with oscillating tunnel barriers, the Coulomb oscillations and staircase are determined by the frequency of the applied rf signals. Figure 1 represents four stages of a rf cycle, where the tunnel barriers oscillate with a phase difference of $\pi$ [14]. In (a) the dashed arrows indicate possible tunneling via the $\mu_d(N+1)$ charge state. For a turnstile operation this tunnel probability must be small because it produces an unwanted leakage current. When the left barrier is reduced, the probability for the $N+1$ electron to tunnel into the dot is strongly enhanced, as illustrated by the solid arrow in (b). Simultaneously, the increase of the right barrier suppresses the probability to tunnel out of the dot to virtually zero. Tunneling into the dot of a second electron is prevented by the Coulomb blockade. At half the cycle time, shown in (c), the barriers are in their equilibrium position again, but compared with (a), one extra electron is confined in the dot. The $N+1$ electron tunnels out when the right barrier is reduced, and simultaneously, the left barrier is increased, which is illustrated in (d). Completing the cycle yields the situation shown in (a), and exactly one electron has passed through the quantum dot. Repeating this process with a frequency $f$ results in a current $I=ef$. Increasing the bias voltage, thereby increasing the number $n$ of charge states contained in the energy interval between $\mu_l$ and $\mu_r$, produces a quantized current $I=nef$, corresponding to frequency-determined current steps in the Coulomb staircase. The steps in the staircase come at voltage intervals of $e/C$, from which we expect an average conductance $\langle G\rangle=ef/(e/C)=fC$.

The accuracy of this quantized current can be estimated by comparing the tunnel times of leakage and wanted events with the rf frequency. In the experiments, we have chosen gate voltages such that the tunnel resistances without applying rf are about 100 GΩ, which yields a

typical leakage time $RC|_{\text{leak}}=10^{-5}$ s. When rf is applied, the minimum of the barrier has a tunnel resistance of order MΩ, yielding a tunnel time for wanted events of $RC|_{\text{tunnel}}=10^{-10}$ s. If $f=10$ MHz, the time ratio $(1/f)/RC|_{\text{leak}}=10^{-2}$ gives a probability for leakage per cycle of $1-e^{-0.01}\approx 0.01$, while $(1/f)/RC|_{\text{tunnel}}=10^{3}$ gives a probability for wanted tunnel events of $1-e^{-1000}\approx 1$. The thermal energy $k_B(10\text{ mK})$ is 2 orders of magnitude less than $e^2/C$, so that excess electron transport via thermal activation is exponentially suppressed. These considerations predict a turnstile accuracy of 1%, somewhat better than that observed in the data presented below.

In Fig. 2 we show measured $I$-$V$ characteristics with 10-MHz signals with a phase difference of $\pi$ applied to QPC gates 1 and 2. The quantized current values $nef$ are indicated by dotted lines [$e(10\text{ MHz})=1.6$ pA]. The curves correspond to different center-gate voltages, and are offset from each other by $ef$. [The gate voltages are $F=-700$ mV, $\text{QPC}_1=-865$ mV, $\text{QPC}_2=-825$ mV, and $C$ ranges between $-500$ and $-504$ mV (uppermost curve) in steps of 1 mV. The rms amplitude of the rf voltages is about 10 mV.] Without rf, the current is less than 0.1 pA between $V=-2$ and $V=3$ mV (not shown). Figure 2 shows that on applying rf, *the $I$-$V$ curves have current plateaus at integer multiples of $ef$, demonstrating that a discrete number of electrons pass through the quantum dot each rf cycle.* Some of the plateaus are missing or weakly developed. Note that this always occurs for two neighboring plateaus. This plateau averaging occurs for roughly equal tunnel barriers: The bias voltage drops across both barriers instead of dropping mainly over one barrier, as required for a well-developed staircase [1].

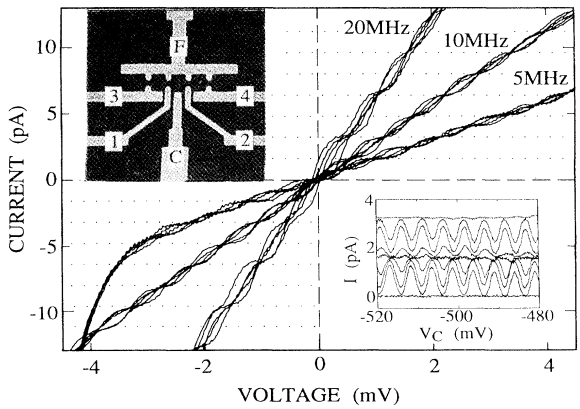


FIG. 3. Main figure: $I$-$V$ curves for rf frequency $f=5$, 10, and 20 MHz, demonstrating scaling with frequency. Dotted lines indicate multiples of $ef$ for $f=10$ MHz. Upper inset: Gate geometry. Lower inset: Current vs center-gate voltage for $f=10$ MHz and different fixed bias voltages. The current oscillations have a frequency-determined amplitude in the interval between $nef$ and $(n+1)ef$.

The current plateaus are illustrated in Fig. 3, where for $f=10$ MHz the same curves are shown as in Fig. 2, but now without offsets. The dotted lines indicate the quantized current values $nef$ for $f=10$ MHz. As expected from the model, the curves have crossings that occur at current multiples of $ef$ and voltage multiples of $e/C$, for $n$ between $-7$ and 7. To demonstrate scaling with frequency, we also show $I$-$V$ curves for $f=5$ and 20 MHz, which have, respectively, twice and half as many crossings as the curves for 10 MHz. Moreover, the average conductance $\langle G\rangle=fC$ scales with frequency, and is in agreement with the value for $C$ obtained from the Coulomb staircase shown in the lower inset of Fig. 2. An alternative way of measuring the same curves is shown in the lower inset of Fig. 3, where the current is plotted versus center-gate voltage for different bias voltages and $f=10$ MHz. The current is independent of center-gate voltage and equal to $nef$ when the bias voltage corresponds to a crossing in the $I$-$V$ curves. In between, the current oscillates with a period equal to that of the Coulomb oscillations shown in the upper inset of Fig. 2. However, the amplitude is now determined by the frequency and lies in the interval between $nef$ and $(n+1)ef$. An analogous result was obtained for the metal turnstile of Ref. [3].

To examine the dependence of the current plateaus on rf amplitude, we measured $I$-$V$ curves for $f=10$ MHz and fixed rf amplitude on $\text{QPC}_2$. The RF amplitude on $\text{QPC}_1$ is increased in constant steps from the uppermost curve in Fig. 4 to the lowest curve. Figure 4 shows that for the same center-gate voltage, all the plateaus from $n=-7$ to 7 are made visible by changing the rf amplitude on one QPC gate. A striking feature is that at zero voltage a nonzero current is observed, which can be either positive or negative. This is due to the influence of the rf signal on the conduction-band bottom of the dot. For

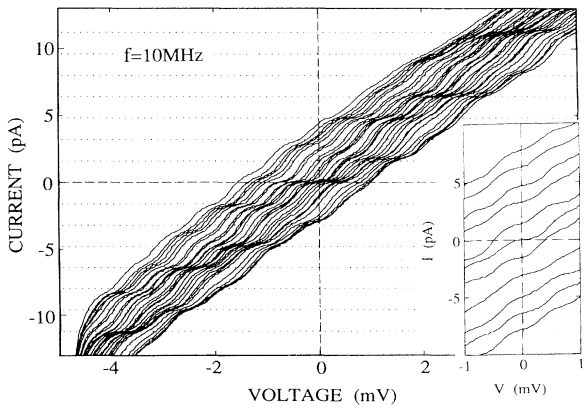


FIG. 4. $I$-$V$ characteristics with fixed rf amplitude on $\text{QPC}_2$ and different rf amplitudes on $\text{QPC}_1$, showing all the current plateaus from $-7ef$ to $7ef$. Inset: $I$-$V$ characteristics with current plateaus from $-5ef$ to $5ef$ at zero bias voltage, demonstrating discrete electron pumping.

equal rf amplitudes on the two QPCs and phase difference $\pi$, this influence is compensated, so the band bottom does not move, and consequently $I(V=0)=0$. However, for unequal rf amplitudes, charge states can be pumped to higher energy. For instance, in Fig. 1(d), a large increase of the left barrier will lift the state $\mu_d(N)$ above $\mu_r$, resulting in an extra electron passing through the quantum dot per rf cycle. Similar arguments explain the pumping around zero voltage and predict the direction of the pumped current, which is found to be in agreement with the measurements. A plot similar to Fig. 4 was obtained by varying the phase difference between compensating rf signals, instead of varying one rf amplitude.

From these measurements, we have been able to deduce the effect on the quantized current plateaus of the center-gate voltage, the rf amplitudes, and the phase difference. To demonstrate the tunability of the quantum-dot turnstile, we have measured the pumping in more detail, which is shown in the inset of Fig. 4. Tuning the different parameters, *we found quantized current plateaus from $n=-5$ to 5 around zero voltage, showing that a discrete number of electrons are pumped per rf cycle.*

In summary, we have realized a quantum-dot turnstile using oscillating tunnel barriers. The observation of quantized current plateaus at multiples of $ef$ demonstrates the ability to control current on a single-electron level.

We wish to thank L. J. Geerligs, K. K. Likharev, J. E. Mooij, and B. J. van Wees for stimulating discussions, A. van der Enden, W. Kool, and D. J. Maas for the device fabrication, and the Delft Institute for MicroElectronics and Submicrontechnology for the use of their facilities. Financial support from FOM and ESPRIT (Project No. 3133, NANSDEV) is gratefully acknowledged.

[1] See, for a review, D. V. Averin and K. K. Likharev, in *Quantum Effects in Small Disordered Systems,* edited by B. Al'tshuler, P. Lee, and R. Webb (Elsevier, Amsterdam, 1990).

[2] See, for a recent review, including various semiconductor systems, *Single Charge Tunneling,* edited by H. Grabert, J. M. Martinis, and M. H. Devoret (Plenum, New York, 1991).

[3] L. J. Geerligs *et al.*, Phys. Rev. Lett. **64**, 2691 (1990).

[4] H. Pothier *et al.* (to be published).

[5] Charging experiments on this structure without rf signals are reported by L. P. Kouwenhoven *et al.*, in "Festkörperprobleme/Advances in Solid State Physics, Vol. 31," Proceedings of the German Physical Society Meeting, Münster, 1991 (to be published).

[6] L. I. Glazman and R. I. Shekhter, J. Phys. Condens. Matter **1**, 5811 (1989).

[7] H. van Houten and C. W. J. Beenakker, Phys. Rev. Lett. **63**, 1893 (1989).

[8] A. N. Korotkov, D. V. Averin, and K. K. Likharev, Physica (Amsterdam) **165&166B**, 927 (1990).

[9] A. Groshev, T. Ivanov, and V. Valtchinov, Phys. Rev. Lett. **66**, 1082 (1991).

[10] C. W. J. Beenakker, H. van Houten, and A. A. M. Staring (to be published); C. W. J. Beenakker, Phys. Rev. B **44**, 1646 (1991).

[11] D. V. Averin and Yu. V. Nazarov, Phys. Rev. Lett. **65**, 2446 (1990).

[12] U. Meirav, M. A. Kastner, and S. J. Wind, Phys. Rev. B **40**, 5871 (1989).

[13] P. L. McEuen *et al.*, Phys. Rev. Lett. **66**, 1926 (1991).

[14] A. A. Odintsov, Appl. Phys. Lett. **58**, 2695 (1991).

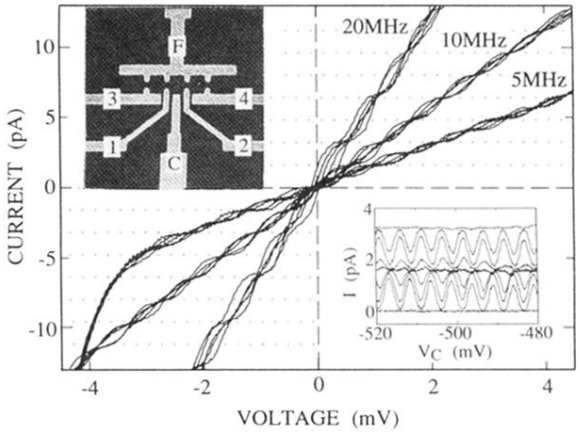


FIG. 3. Main figure: *I-V* curves for rf frequency $f=5$, 10, and 20 MHz, demonstrating scaling with frequency. Dotted lines indicate multiples of $ef$ for $f=10$ MHz. Upper inset: Gate geometry. Lower inset: Current vs center-gate voltage for $f=10$ MHz and different fixed bias voltages. The current oscillations have a frequency-determined amplitude in the interval between $nef$ and $(n+1)ef$.